THERMOELASTIC ANALYSIS OF SANDWICH CONSTRUCTION TEE-JOINTS LOADED IN COMPRESSION

J M Dulieu-Barton[1], J S Grigg[2], R A Shenoi[2], S D Clark[2], and A R Chambers[2]
[1] University of Liverpool, Department of Engineering, Brownlow Hill, Liverpool, L69 3GH
[2] University of Southampton, School of Engineering Science, Highfield, Southampton, SO17 1BJ

SUMMARY: This paper describes experimental work carried out on a variety of sandwich construction tee-joint configurations loaded in compression. The effect of varying the thickness of the laminate that strengthens the joint connection (the boundary angle overlaminate) and the use of a fillet at the connection are examined. Thermoelastic stress analysis is used to determine the stress distribution in the tee-joints by means of the SPATE system. Procedures for calibrating the thermoelastic data are described. The maximum stress values are identified in each of the tee-joint constituents, these are compared with the failure stresses and the implications are discussed in detail. To illustrate the potential of the technique one set of results is compared to finite element data for an identical joint.

KEYWORDS: Thermoelastic Stress Analysis (TSA), SPATE, Sandwich Materials, Foam Construction, Tee-Joints.

INTRODUCTION

Out-of-plane connections in large structures are necessary for adequate stiffness and load distribution around the structure. Tee-joints are of particular relevance in the ship building industry, characterising the connection between the bulkheads and the hull. These joints are constructed using secondary bonds, since they cannot be formed concurrently with the main structure. For this reason there are inherent weaknesses in such joints, primarily due to stress concentrations and a lack of continuity of fibre reinforcement across the bond. It is therefore important to be able to understand the load transfer mechanism within joints of this type. The majority of the work to date has concentrated on single-skin laminated GRP structures. Detailed finite element analysis has successfully lead to the prediction of stress distributions and load transfer mechanisms within joints of various geometries under representative static loads [1]. These have been validated experimentally using thermoelastic and photoelastic stress analysis techniques [2, 3]. This work has been supported by extensive joint testing programmes both under static and cyclic loading conditions, enabling the inception and progression of failure to be determined [4]. More recently, sandwich construction has been employed in smaller vessels. So far the global behaviour of these joints has been determined experimentally under static loading [5, 6] and finite element analysis (FEA) has been carried out. A small amount of work has been done to provide an experimental verification of the FE model using thermoelastic analysis on a tee-joint loaded in a 45° pull-off mode [7].

Thermoelastic stress analysis (TSA) is a well established experimental technique and has been used in a wide range of engineering applications [8]. The technique is based on the measurement of a small temperature change that occurs in solids when they are subjected to elastic cyclic stresses. In isotropic materials the temperature change, ΔT, is directly proportional to the changes in the sum of principal stresses, $\Delta(\sigma_1 + \sigma_2)$, in the structure as follows

$$\Delta T = K\, T\, \Delta(\sigma_1 + \sigma_2) \quad (1)$$

where T is the absolute temperature of the material and K is the thermoelastic constant ($K = \alpha/\rho\, C_p$, α is the coefficient of linear thermal expansion, ρ is the density and C_p is the specific heat at constant pressure of the material).

In orthotropic materials it can be shown [8] that ΔT is not directly proportional to the stresses but to a combination of stresses and αs, i.e.

$$\Delta T = \frac{T}{\rho C_p}\left(\alpha_{11}^{P}\Delta\sigma_{11} + \alpha_{22}^{P}\Delta\sigma_{22}\right) \quad (2)$$

where α_{11}^{P} and α_{22}^{P} are the coefficients of linear thermal expansion in the principal material directions and $\Delta\sigma_{11}$ and $\Delta\sigma_{22}$ are the changes in the direct stresses in the principal material directions.

The equipment used in the thermoelastic work is the SPATE (Stress Pattern Analysis by Thermal Emissions) system [8]. The system contains a highly sensitive infra-red detector which converts the photon emission from the specimen due to the small temperature change into a voltage signal which can be directly related to ΔT and hence the stresses. The technique offers many advantages when studying sandwich construction parts. It is non-contact and therefore does not use attachments that may stiffen the joint. A full-field representation of the stresses can be obtained which permits an immediate visualisation of the stress distribution through the joint and hence the importance of each of the joint constituents in the load transfer process. The resolution of the SPATE system is ca. 0.5 mm which allows more detailed measurement than that given by conventional strain gauges.

It is clear from equation (2) that stress values cannot be obtained directly from thermoelastic data. However, the quantity ΔT is an important stress metric and can be used as a basis for validation. The aim of this paper is to use the thermoelastic stress analysis technique to determine the load transfer mechanisms in sandwich construction tee-joints and to compare the stress sum distributions in a variety of tee-joint constructions. A compression mode of loading has been used in this case, which is applicable to smaller, stiffer marine structures such as lifeboats, which can often be highly loaded in a 'slamming' mode due to wave impacts. This is a more realistic loading mode for this type of structure than the 45° mode reported previously [7], which is typical of the loading experienced by larger craft.

TEST SPECIMENS AND LOADING CONFIGURATION

A diagram of a typical joint used in the thermoelastic work is shown in Figure 1. The joints are constructed from a web of core thickness 50 mm attached to a flange of core thickness 100 mm. The depth of each joint is also 100 mm. The flange and web are 800 mm and 280 mm in length respectively. The materials used in the construction of the joints are cross-linked closed cell PVC foams for the web and flange cores and continuous glass fibre reinforced epoxy laminates for the skins. The flange core is Divinycell H130 of nominal density 130 kg/m^3, and the web core is Divinycell H80 of nominal density 80 kg/m^3. The web skins and flange inner skin are made from a 2 ply 1200 g/m^2 quadriaxial 0/90/±45° E-glass fabric in an epoxy resin matrix. The flange and web are joined directly using an epoxy adhesive (SPX7049/SPX7310). In some cases

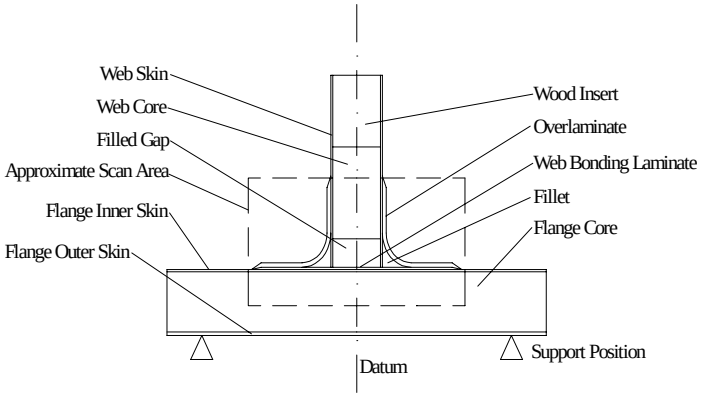

Figure 1: Tee-Joint Construction

a manufacturing variation occurs which causes a gap between the flange and the base of the web which is subsequently filled with a colloidal silica filled epoxy. This material is also used in the formation of fillets at the base of the joint. The joint is completed by the overlaminate which forms a boundary angle between the web and the flange. This material is a 900 g/m^2 ±45° glass fabric in an epoxy matrix, which is also used in the web bonding laminate. The flange outer skin is made from a 1200 g/m^2 E-glass/aramid/epoxy pre-preg. The wood insert is solely for ease of testing. A summary of the relevant material properties is given in Table 1.

One of the aims of this work is to determine the effect of various geometrical and manufacturing differences on the stress distributions in the joints. The variables investigated are the thickness of the overlaminate, the radius of the fillet and the presence of a filled gap. A summary of the six different configurations used in this study is given in Table 2. For the joint with the filled gap, the gap is much larger than would be expected as a result of variations in manufacture, however this is intended to model the worst case.

CALIBRATION OF JOINT CONSTITUENT MATERIALS

As the joint is made up from a variety of materials, each with a different thermoelastic constant, it is necessary to derive a calibration constant, A, [9] for each material; this includes the thermoelastic constant, K, the detector response factor, surface properties and any signal amplification factors. As the foam core is quasi-isotropic then equation (1) can be used as a basis for calibration of this material. It is a straight forward matter to relate the voltage output (i.e. the thermoelastic signal, S) from the SPATE detector to the stress changes [8], i.e.

$$\Delta(\sigma_1 + \sigma_2) = A S \qquad (3)$$

The foam material was calibrated for the previous 45° mode work [7] by using a simple tensile specimen and relating the applied stress, σ_{app}, to the measured signal, i.e. $A = \sigma_{app}/S$. A was derived as 7.07×10^{-4} MPa U^{-1} for the flange core and 2.89×10^{-4} MPa U^{-1} for the web core (where U = uncalibrated signal unit). As identical materials were used in both the 45° pull-off work and the present work, these values were used to calibrate the readings from the foam. (The only difference was that in the 45° work the signal amplification factor was half that used in the current work so it was necessary to double the A values).

Table 1: Tee-Joint Material Properties

Component	Tensile Modulus (MPa)	Compressive Modulus (MPa)	Shear Modulus (MPa)	Tensile Strength (MPa)	Compressive Strength (MPa)	Poission's Ratio
Web Core	75	32	31	1.95	1.0	0.32
Web Skins	20707		7450			0.28
Flange Core	140	85	52	4.20	2.5	0.32
Flange Inner Skin	20707		7450	310		0.28
Overlaminate	14400		4500	216		0.10
Filet Resin	3300		3500	85		0.37

Table 2: Tee-Joint Configurations

Specimen Number	No. of Plies in Overlaminate	Fillet Radius (mm)	Filled Gap Size (mm)
1	4	0	0
2	2	0	0
3	4	30	0
4	2	30	0
5	2	30	25
6	0	30	0

The boundary angle overlaminate is an orthotropic material in the through-thickness plane. It is therefore necessary to use equation (2) as a basis for calibration. In order to obtain a simple expression for calibration purposes two constants are introduced [2]; A*, similar to A but not including the αs and $\alpha^* = \alpha_{22}^P / \alpha_{11}^P$. Using these constants an expression for the relationship between the thermoelastic signal and the stress changes is obtained as follows [2]:

$$\Delta\sigma_{11} + \alpha^* \Delta\sigma_{22} = A^* S \qquad (4)$$

A* is required to calibrate the thermoelastic data and α* is required for comparing the thermoelastic data with finite element analysis. As manufacturers values for material constants for GRP are unavailable, an experimental means of deriving the constant is required. To obtain A* some of the boundary angle material, $\pm 45°$ glass fabric, was manufactured into laminated flat strips of 200 mm in length by 10 mm thick by 50 mm wide. The strips were loaded in tension as shown in Figure 2, to levels of 6 ± 2 kN and 6 ± 4 kN. The direction of the applied load corresponded to the principal material direction 11 so that $\Delta\sigma_{11} = \Delta\sigma_{app}$ and $\Delta\sigma_{22} = 0$. Therefore A* can be obtained from equation (4) by the following

$$\frac{A^*}{S} = \Delta\sigma_{app} \qquad (5)$$

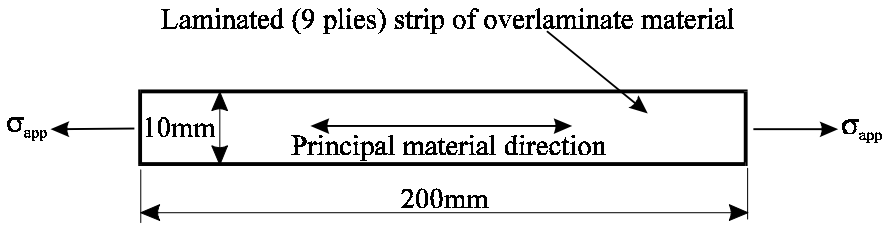

Figure 2: A calibration specimen*

SPATE scans were taken from the four strips and A* values were obtained from four specimens for both load ranges. An average A* value was calculated as 16.05×10^{-3} MPa U^{-1}; there was considerable scatter in the data, the coefficient of variation being around 14%. However, this was due to the variation of the material and not due to any non-linear behaviour as the A* values at the two loads were identical for each specimen.

To calibrate α^*, $\Delta\sigma_{11}$ must be eliminated in equation (4). In order to achieve this two specimens were constructed from nine pieces of 30 mm by 30 mm by 10 mm thick laminated ± 45° glass fabric material as shown in Figure 3. The specimens were loaded in compression to a level of 8 ± 6.5 kN so that $\Delta\sigma_{22} = \Delta\sigma_{app}$ allowing equation (4) to be rewritten as

$$\frac{\alpha^*}{\Delta\sigma_{app}} = A^*S \qquad (6)$$

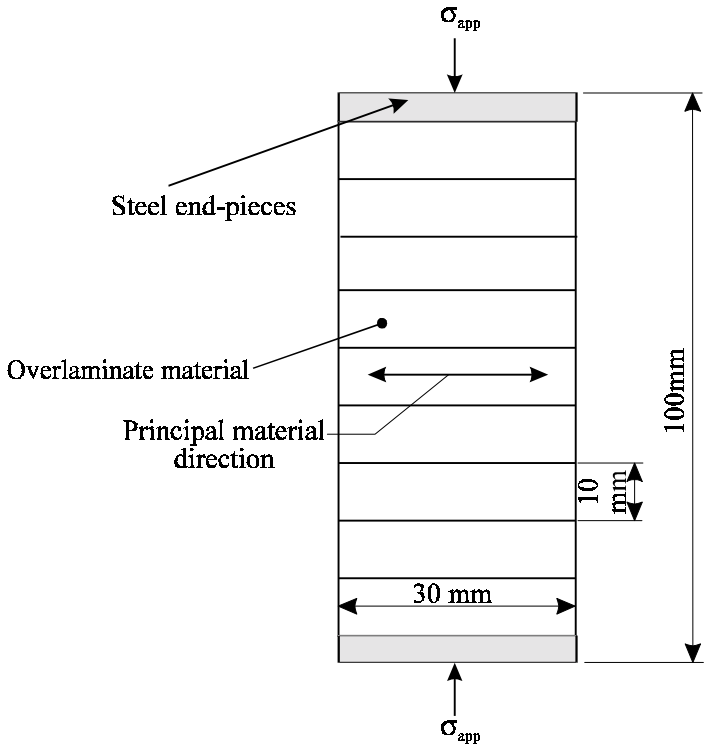

Figure 3: α calibration specimen*

SPATE readings were taken from the four faces of each specimen. Once again because of the laminated construction of the individual 30 mm × 30 mm pieces there was much scatter in the average signal, which was –1421 U with a coefficient of variation of 11%. This average signal value was used in equation (6) along with the A* value determined previously to give an α^*

value of 1.61. This value may seem low as it would be expected that α_{22}^{P} would be greater than α_{11}^{P} for most composite materials. However, in this through-thickness mode the influence of the fibres will be small as the in-plane lay-up is ± 45°. A more isotropic behaviour would therefore be expected as only an elliptical cross section of the fibre would be influencing the response in the plane of scanning. In the current work the assumption has been made that the 0/90°/± 45° quadriaxial E-glass in the place of scanning skin material was the same A* and α value as the overlaminate. This is clearly just an estimation and further calibration work needs to be conducted to confirm this. However, for the purposes of comparing the order of the skin stresses to the foam stresses this is a useful assumption.

The fillet material was calibrated using the detector and material properties [9], i.e.

$$A = \frac{DGR}{Te2048\,K} \tag{7}$$

where D is the detector response factor, G/2084 is an amplification factor, R is a temperature correction factor and for readings taken other than at 20°C, T is the temperature of the surface of the material and e is the surface emissivity. D for the detector used in the current work is 12.9 KV^{-1}, G was set to 10mV, T was taken to be 293 K, therefore R = 1 and e was 0.92. The density of the fillet material was calculated using a rule of mixtures approach as 1161 kgm^{-3}, α was calculated assuming that the particulate behaves in a similar way to a 90° construction in the through-thickness direction, this approach gave $\alpha = 59.1 \times 10^{-6}$ and C_p was taken as the value for the pure resin, i.e. 3000 J $kg^{-1}K^{-1}$. These gave a K value of 16.9×10^{-1} MPa^{-1} and substituting all the above into equation (7) gave an A value of 12.9×10^{-3} MPa U^{-1}.

EXPERIMENTAL WORK

The tee-joints were simply supported by rollers spaced 350 mm apart symmetrically about the centreline of the web on the flange outer skin (see Figure 1). A compressive load was applied directly to the end of the web (in the plane of the web) using a hydraulic ram. For the thermoelastic tests the applied load was 650 ± 3.4 kN at a frequency of 8 Hz. The approximate SPATE scan area is shown in Figure 1. The SPATE detector was set at a working distance of 960mm giving a scanning spot size of 1.23mm with a resolution of 1.44 mm. Each scan took approximately 2 hours to complete. The data was calibrated using the calibration constants given in the previous section. (To do this the SPATE data was exported to a spreadsheet package, the data from the different constituents were identified and then multiplied by the relevant A or A* value.) Two line plots were taken through the data. One through the flange core 2 mm below and parallel to the inner skin. The other horizontally across the web at the top of the fillet. The two line plots for joint number 4 are shown in Figure 4.

The maximum value from each of the line plots is given in Table 3. Along with the position of the maxima. The datum was taken as the centre line of joint and position values to the left of the datum are indicated in Table 3 by a minus sign. The joints are nominally symmetrical, so therefore the stresses either side of the datum line should be symmetrical. It is clear from Table 3 that this is not the case and illustrated quite clearly in Figure 4a where the stress sum values for the flange are greater on the left of the plot. This is because of inaccuracies in the manufacturing process and in the loading. There is, in most cases, a reasonable correspondence between the maximum values either side of the joint. The most antisymmetric of the values are those from specimen 5 (i.e. the joint with a filled gap). On inspection of this joint it was found that the filler was non-uniform through the thickness of the joint.

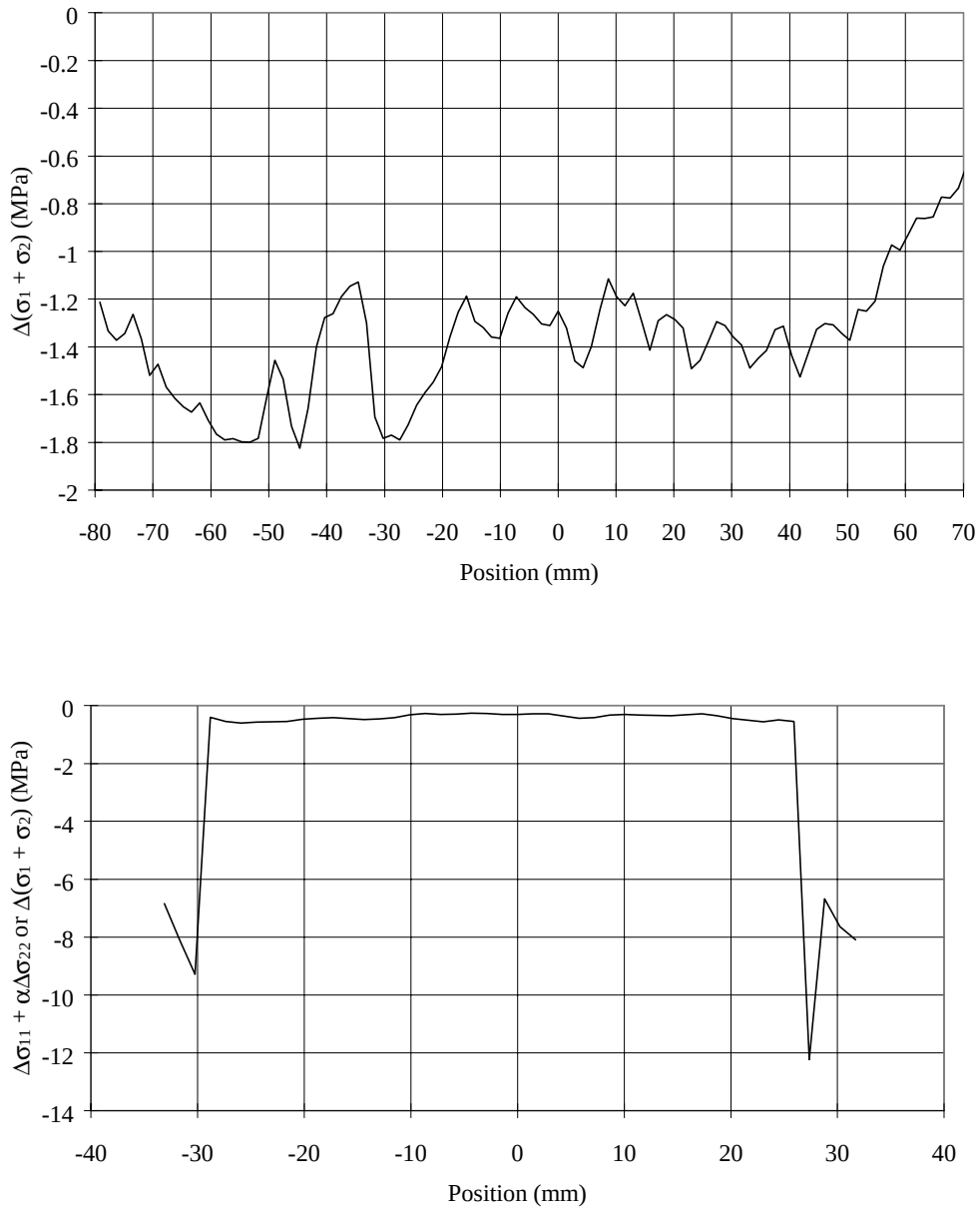

Figure 4: SPATE line plots through (a) flange and (b) web

In the flange core the maximum stress sum value occurs at a point in-line with the position of the web skins for the joints without a fillet (specimens 1 and 2). The greatest stress sum values occur in the flange core in the overlaminated joints without a fillet. The addition of the fillet has a beneficial effect on the stress sum values in the flange core, causing the load to be more spread and the maxima occurring beyond the plane of the web. The use of the overlaminate also has a beneficial effect on the stresses in the flange core; the greatest value of stress sum was recorded in joint 6 (i.e. no overlaminate) with decreasing values for joint 4 (2 plies) and joint 3 (4 plies). The lowest value of stress sum in the flange core is given by joint 5, which contained the filled gap. The compressive failure strength of the flange core material is 2.5 MPa (see Table 1), the maximum stress sum values in joints 1, 2, 6 either approach or exceed this under these loading conditions. Therefore the use of an overlaminate and a fillet must be regarded as essential to prevent flange core failure.

Table 3: Maximum values determined from calibrated SPATE data

Specimen Number	Flange Core		Web Core		Overlaminate/Web		Fillet	
	$\Delta(\sigma_1+\sigma_2)$ (MPa)	Position (mm)	$\Delta(\sigma_1+\sigma_2)$ (MPa)	Position (mm)	$\Delta\sigma_{11}+\alpha\Delta\sigma_{22}$ (MPa)	Position (mm)	$\Delta(\sigma_1+\sigma_2)$ (MPa)	Position (mm)
1	-2.1	-16	-0.30	-24	-4.2	-27	-	-
	-2.6	27	-0.30	26	-7.2	30	-	-
2	-2.5	-23	-0.29	-26	-5.1	-29	-	-
	-2.0	33	-0.28	27	-4.1	29	-	-
3	-1.4	-40	-0.44	-30	-10.0	-36	-9.3	-35
	-1.3	24	-0.38	22	-7.1	36	-7.2	39
4	-1.8	-45	-0.60	-29	-9.3	-30	-7.5	-33
	-1.5	42	-0.66	23	-12.2	27	-7.0	29
5	-1.4	-69	-0.26	-27	-5.6	-30	-10.0	-43
	-0.8	49	-0.23	29	-5.0	32	-6.1	50
6	-2.8	-17	-0.79	-26	-18.3	-27	-17.3	-29
	-2.2	29	-0.70	26	-15.1	27	-16.7	29

The maximas in the web core occurred adjacent to the web skin. When there is no fillet, i.e. specimens 1 and 2, the stress sum maximum is less than that given for joints with a fillet, i.e. specimens 3 and 4. An increase in the overlaminate thickness has a beneficial effect on the web core stresses for specimens with fillet but a negative effect on the joints without a fillet. The maximum stress sum value was recorded in Specimen 6, i.e. no overlaminate, and the minimum in the joint with a filled gap, i.e. specimen number 5. The compressive failure strength of the web core is 1.0 MPa (see Table 1); this was not exceeded in any of the tests.

The maximum $\Delta\sigma_1 + \alpha * \Delta\sigma_2$ values occur in positions that correspond to the web skin, with exception of specimen 3 where the maximum occurs in the boundary angle overlaminate. A comparison of the $\Delta\sigma_1 + \alpha * \Delta\sigma_2$ values with maximum tensile strength values given in Table 1 show that the overlaminate and the flange skin are not close to their failure loads. (At present it is difficult to judge the influence of α^* on the data and this will be dealt with elsewhere.) Assuming that the compressure strength of the laminates is of the order of 80% of the quoted tensile strengths given in Table 1, then it is clear that the stresses in the overlaminate and the skin are only a fraction of the failure strength of the materials, whereas the stresses in the cores are approaching or beyond the quoted failure strength of the foam, thus indicating that failure of the foam will play an important role in the integrity of the joint.

In the joints with the fillet it is interesting that the fillet carries a substantial amount of stress, particularly when there is no overlaminate. Although, in these tests the stress sum values are much less than the failure load, it is evident that with increasing loads the fillet would be the second constituent to fail after the core.

Most surprising of all the results is the beneficial effect that a filled gap has on the stresses in all the constituents. The local stiffening effect of resin (i.e. 100 fold increase compared to the stiffness of the web) must be responsible for the reduction. The effect clearly warrants further investigation.

DISCUSSION

Some previous work has been carried out on these types of joint under static loading [5]. Compression failure was observed in the web and flange cores, characterised by a bulging of the foam. In the case of the flange, this was in the area contacted by the web skins, in the position shown to contain the maximum stress in the SPATE work. As the load was increased the joints exhibited a progressive accumulation of damage, with the majority of the strength degradation occurring after the initial failure of the fillet resin. The thermoelastic work showed that the stresses were high in the fillet in comparison to its failure load and this finding is therefore supported by the initial static loading study. After the fillet failure, cracking occurred through the thickness of the overlaminate accompanied by delamination and fibre buckling. Buckling was also observed in the top skin of the flange adjacent to the areas identified in the SPATE work as having maximum stresses. The maximum in-plane stresses in the overlaminate and the skins were not large enough to cause this failure. This is substantiated by the SPATE work which shows small stress values in these constituents compared to the quoted failure stress values. It is clear that an interlaminar tensile stress large enough to cause delamination must exist. This is not apparent in any of the SPATE plots because the resolution of the equipment is not high enough to detect this very localised effect. A new equipment for themoelastic stress analysis known as the Deltatherm System [8] is now available and uses an array of detectors. It is possible to obtain resolutions of the order of 0.01 mm by using specially designed lenses with this equipment. Therefore future work will concentrate on studying the laminates in the level of detail necessary to identify the interlaminar tensile stresses. A further feature which must play a role in the joint failure is the adhesive bond between the skins and core; the high resolution lens the will also permit the study of this. The current work has shown the important role of the foam core in the failure of the joint and early failure of the foam will also contribute to the buckling of the skins. Also the work has shown that the existence of a fillet has clear beneficial effects on the stresses in the joint and carries a substantial amount of the load. The use of an overlaminate has shown to be essential in minimising the stresses in all the parts of the tee-joint.

Some FEA has been carried out on joint 4. The experimentally derived value of α^* was used to convert the FEA to a form identical to that of the SPATE data. A maximum $\Delta\sigma_1 + \alpha^* \Delta\sigma_2$ value of –11.3 MPa was recorded in the web skin which corresponds very well to the average of the SPATE data of –10.8 MPa. However, the FEA recorded a much larger value in the overlaminate of –17.6 MPa compared to a value of –8.0 MPa given by the SPATE data. This could be attributed to edge effects which have been shown [10] to cause a reduction in readings at an edge. The flange core FEA values were also 50% smaller than those obtained from the SPATE readings, this may be attributed to some inaccuracies in the material constants included in the finite element regime. This theory is strengthened by the fact that the web core values were much closer, i.e. –0.47 MPa from the FEA compared to an average of -0.63 from SPATE. Although the correlation between the FEA and the SPATE data can only be regarded as moderate an examination of the actual $\Delta\sigma_1 + \alpha^* \Delta\sigma_2$ distributions is very encouraging, the "shape" of the distribution is virtually identical indicating a deficiency in the material properties used in the FEA.

CLOSURE

TSA has been successfully used in a comparison of stresses in a variety of tee-joint configurations. This has allowed the importance of each of the tee-joint constituents to be identified in terms of stress reduction and load transfer. The work has shown that under this compression loading mode stresses can be developed in the foam that are in excess or

approaching failure stresses. The introduction of a fillet and the use of an overlaminated boundary angle reduce the stresses considerably. The work has demonstrated the versatility of the thermoelastic technique and its applicability to real complex composite structures.

REFERENCES

1. Shenoi, R.A. and Hawkins, G.L., "Influence of Material and Geometry Variations on the Behaviour of Bonded Tee Connections in FRP Ships", *Composites*, Vol. 23, No. 5, 1992.

2. Dulieu-Smith, J.M., Quinn, S., Shenoi, R.A., Read, P.J.C.L. and Moy, S.S.J., "Thermoelastic Stress Analysis of a GRP Tee-Joint", *J. Applied Composite Materials*, Vol. 4, No. 5, 1997, pp 238-303.

3. Read, P.J.C.L., Dulieu-Smith, J.M. and Shenoi, R.A., "Thermoelastic and Photoelastic Analyses to Characterise Stresses in FRP Connections", *Proc. Int. Conf. on Composite Materials*, 1996, Durban, pp 415-420.

4. Shenoi, R.A., Read, P.J.C.L. and Hawkins, G.L., "Fatigue Failure Mechanisms in Fibre Reinforced Plastic Laminated Tee-Joints", *International Journal of Fatigue*, Vol. 17, No. 6, 1995, pp 415-426.

5. Hicks, I.A., Read, P.J.C.L. and Shenoi, R.A., "Tensile Compressive and Flexural Characteristics of Tee-Joints in Foam-Cored Sandwich Structures", *Proc. 3rd Int. Conf. Sandwich Construction*, 1995, Southampton, pp 579-590.

6. Shenoi, R.A., Read, P.J.C.L. and Jackson, C.L., "Influence of Joint Geometry and Load Regimes on Sandwich Tee-Joint Behaviour", *J. Reinforced Plastics and Composites*, Vol. 17, No. 8, 1998, pp 725-740.

7. Dulieu-Smith, J.M., Read, P.J.C.L. and Shenoi, R.A., "Thermoelastic Analysis of Foam-Cored Sandwich Construction Tee-Joints", *11th Int. Conf. on Composite Materials*, Gold Coast, 1997, pp 699-708.

8. Dulieu-Barton, J.M. and Stanley, P., "Development and Applications of the Thermoelastic Stress Analysis Technique", *J. Strain Analysis*, Vol. 33, No. 2, 1998, pp 93-104.

9. Dulieu-Smith, J.M., “Alternative Calibration Techniques for Quantitative Thermoelastic Stress Analysis”, *J. Strain Analysis*, Vol. 31, No. 1, 1995, pp 9-16.

10. Barone, S., “A Technique for Smoothing Interior Thermoelastic Data and Enhancing Boundary Information”, *Strain*, Vol. 33, No. 1, 1997, pp 9-13.